PROBLEMS ASSOCIATED WITH OBTAINING ACCURATE DYNAMIC STABILITY RESULTS FROM FREE-FLIGHT TESTS*

Gary T. Chapman and Donn B. Kirk

National Aeronautics and Space Administration
Ames Research Center
Moffett Field, Calif.

INTRODUCTION

To obtain dynamic stability results from ballistic range flight tests, angular orientation measurements at discrete points along the trajectory are used to evaluate parameters in the solutions to various equations of motion. A number of factors combine to degrade the derived dynamic stability result. First, the apparent damping of the motion can be significantly influenced by errors that are made in measuring angles from photographs of the model in flight. And second, the equations of motion are influenced by the approximations that are made in both setting up the equations and in solving them.

This paper will cover some phases of each of these problems. We will first review the data reduction procedure presently in use at Ames. Then the effect of experimental errors on dynamic stability results will be considered, first from a simple theoretical standpoint, then from a statistical approach involving perturbations of exact solutions.

Finally we will consider two assumptions involving the equations of motion which can give rise to errors: (1) The assumption that the

*Prepared for the Second Technical Workshop on Dynamic Stability Testing, Arnold Engineering Development Center, April 20-23, 1965.

resultant angle of attack is the square root of the sum of the squares of the two orthogonal projected angles, and (2) the assumption that a linear restoring moment and constant damping coefficient govern the model oscillation. Exact trajectories will be computed and then analyzed by our existing data reduction procedure. Typical examples will be shown to demonstrate the magnitude of errors that can be expected, and ways of eliminating or minimizing these errors will be discussed.

SYMBOLS

A	reference area
$a_1, \ldots, a_6$	constants in equations (1)
C_D	drag coefficient
C_{L_α}	lift-curve slope
C_m	pitching-moment coefficient
C_{m_α}	pitching-moment curve slope
$C_{m_q} + C_{m_{\dot{\alpha}}}$	rate of damping in pitch
d	reference diameter
I_y	moment of inertia about pitch axis
k	constant $\rho A/4m$
M_0, M_2	constants used to define nonlinear restoring moment curves
m	model mass
N	number of observation points per cycle

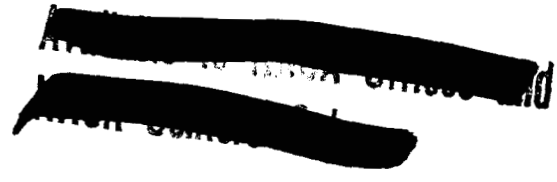

n	number of cycles of motion
p	roll rate
$SD\alpha$	standard deviation in angle of attack due to experimental errors
$SD\xi$	standard deviation in ξ
x	distance along flight path
α,β	angles of attack and sideslip
α_r	resultant angle of attack
$\Delta\alpha$	change in pitch amplitude due to damping
Δx	distance between observation stations
$\eta,\eta_2,\omega,\omega_2$	constants in equations (1)
λ	wave length of pitching oscillation
ξ	dynamic stability parameter defined in equation (3)
ρ	air density
σ	radius of gyration of model about pitch axis
φ	angle between observation plane and plane of motion

Subscripts

E	exact value
env	envelope
env_o	envelope at $x = 0$
i	individual readings
RMS	root mean square

DATA REDUCTION PROCEDURE

The current data reduction procedure consists of curve-fitting measured values of α, β, and x (this is where experimental errors enter the problem) with a solution to the equations of motion. This solution is the tricyclic solution of Nicolaides (ref. 1), transformed to distance (x) rather than time (t) dependence. This solution allows for constant roll rate and small asymmetries. The solution is

$$\alpha = e^{\eta_1 x}(a_1 \sin \omega_1 x + a_2 \cos \omega_1 x) + e^{\eta_2 x}(a_3 \sin \omega_2 x + a_4 \cos \omega_2 x) + (a_5 \sin px + a_6 \cos px) \tag{1a}$$

$$\beta = e^{\eta_1 x}(a_1 \cos \omega_1 x - a_2 \sin \omega_1 x) - e^{\eta_2 x}(a_3 \cos \omega_2 x - a_4 \sin \omega_2 x) + (a_5 \cos px - a_6 \sin px) \tag{1b}$$

where the constants $\omega_1, \omega_2, \eta_1, \eta_2, a_1, \ldots, a_6$ are determined by the curve-fitting procedure (p, the roll rate, is related to ω_1 and ω_2); the curve fitting is carried out by a differential correction procedure. The dynamic stability parameter is related to η_1 and η_2 as follows:

$$\xi = \frac{2m}{\rho A}(\eta_1 + \eta_2) \tag{2}$$

where ξ is the constant-altitude power-off dynamic stability parameter related to the aerodynamic coefficients by

$$\xi = C_D - C_{L_\alpha} + \left(C_{m_q} + C_{m_{\dot{\alpha}}}\right)\left(\frac{md^2}{I_y}\right) \tag{3}$$

The static stability parameter C_{m_α} is related to ω_1 and ω_2 as

$$C_{m_\alpha} = \frac{-2\omega_1\omega_2 I_y}{\rho A d} \tag{4}$$

The major assumptions employed in the derivation of equations (1) which give rise to apparent errors, particularly in the dynamic stability parameter, are: (1) the aerodynamic coefficients are assumed to be constants or linear functions of angle of attack; and (2) the resultant angle of attack α_r is assumed to be given as $\alpha_r = \sqrt{\alpha^2 + \beta^2}$ instead of $\tan^{-1}\sqrt{\tan^2 \alpha + \tan^2 \beta}$. The systematic errors generated by these assumptions usually appear as an absolute shift in the results as contrasted to random errors arising in the experimental measurements of α, β, and x. These two sources of error will be treated independently.

ANALYSIS OF RANDOM EXPERIMENTAL ERRORS

A statistical analysis will be presented, which consists of calculating exact trajectories, introducing simulated experimental errors via a Monte Carlo procedure, and analyzing these perturbed trajectories with the data reduction procedure just described. For simplicity we will consider linear aerodynamics and planar motion in calculating the exact trajectories. However, before proceeding further a brief look at a simplified version of the problem will help in interpreting the statistical results and provide some guidelines as to what variables might be important.

Simple Theory

We will consider the error involved in determining the dynamic stability parameter from two data points which represent points on the envelope of the pitching motion (see sketch (a)). The equation for the envelope of the arc is given as

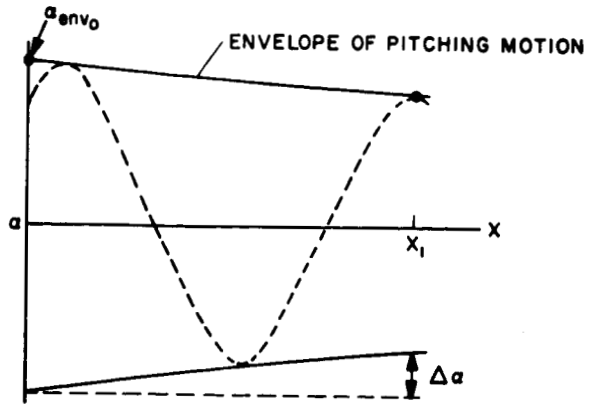

Sketch (a)

$$\alpha_{env} = \alpha_{env_o} e^{k\xi x} \tag{5}$$

where $\alpha_{env_o} = \alpha_{env}$ at $x = 0$, and $k = \rho A/4m$. Equation (5) can be rewritten as

$$\ln\left(\frac{\alpha_{env}}{\alpha_{env_o}}\right) = k\xi x \tag{6}$$

If we now take two data points at $x = 0$ and x_1 and write α_{env_1} as

$$\alpha_{env_1} = \alpha_{env_o} + \Delta\alpha$$

equation (6) becomes

$$\ln\left(1 + \frac{\Delta\alpha}{\alpha_{env_o}}\right) = k\xi x_1 \tag{7}$$

If there is now some error in determining α_{env} at each point (the probable error at each point can be represented as $SD\alpha$),[1] then $\Delta\alpha$ is determined to within $\sqrt{2}\ SD\alpha$ and therefore there will be some probable error in ξ, noted as $SD\xi$. From these ideas we can write equation (7) as

---

[1]SD refers to standard deviation and has its usual statistical definition $SD\alpha = \sqrt{\frac{1}{n}\sum_{i=1}^{n}(\alpha_i - \alpha_E)^2}$ where α_i are individual readings, α_E is the exact value, and n is the number of readings.

$$\ln\left(1 + \frac{\Delta\alpha}{\alpha_{env_o}} + \frac{\sqrt{2}\ SD\alpha}{\alpha_{env_o}}\right) = k(\xi_E + SD\xi)x_1 \tag{8}$$

If

$$\frac{\Delta\alpha}{\alpha_{env_o}} + \frac{\sqrt{2}\ SD\alpha}{\alpha_{env_o}} < 1$$

we can expand the logarithm, and to first order we get

$$\frac{\Delta\alpha}{\alpha_{env_o}} + \frac{\sqrt{2}\ SD\alpha}{\alpha_{env_o}} \simeq k(\xi_E + SD\xi)x_1 \tag{9}$$

We can now associate exact and error terms such that the $SD\xi$ can be expressed as

$$SD\xi \simeq \sqrt{2}\ \frac{SD\alpha}{\alpha_{env_o}}\ \frac{1}{kx_1} \tag{10}$$

If we now consider x_1 to be located at the end of the observed trajectory and replace x_1 by $n\lambda$, where n is the number of cycles and λ is the wave length of the pitching motion, we get

$$SD\xi \simeq 4\sqrt{2}\left(\frac{SD\alpha}{\alpha_{env_o}}\right)\left(\frac{m}{\rho A\lambda}\right)\left(\frac{1}{n}\right) \tag{11}$$

Equation (11) gives an indication of what to expect from a statistical analysis. Note that this equation states that $SD\xi$ does not depend on ξ. This fact will be used to simplify the analysis; however, it will also be checked for validity by comparison with some statistical results.

Note that equation (11) tells nothing about the effect of the number of data points considered. Therefore, in addition to the parameters given in equation (11), we will also consider the number of observation points per cycle (N) defined as $N = \lambda/\Delta x$, where Δx is the distance between observation stations. Note that the total number of observation stations is given as $nN + 1$.

Statistical Analysis

The procedure that was followed was to assume an arbitrary set of linear aerodynamic coefficients $\left(C_{m_\alpha},\ C_{m_q} + C_{m_{\dot{\alpha}}},\ \text{etc.}\right)$ and generate at discrete points a number of planar trajectories (we will refer to these trajectories as a group). In this group, the only variation was the position of the first station relative to the first maximum in the angle of attack; that is, the phase relationship between observation stations and the motion history was varied. A Monte Carlo technique was then used to introduce errors in both the angle and distance readings, simulating experimental errors. In most cases, a uniform error distribution was used, but several cases were investigated using a normal error distribution as well. This group of trajectories was then analyzed with the existing data reduction procedure and the standard deviations in the parameters of interest were determined (e.g., SDξ and SDλ). This process was repeated for different groups varying the values of SDα, α_{RMS}, $m/\rho A\lambda$, ξ, n (number of cycles), and N (number of data points per cycle).

Before considering the results, however, we must decide how many trajectories will form a meaningful statistical sampling. This question was considered in a reverse manner as follows. It was felt that perhaps 20 independent trajectories would be sufficient to be statistically meaningful. To check this, three different groups of 22 runs each (allowing for the possibility of rejecting several ill-conditioned runs) were statistically analyzed and compared, and it was felt if

each of the three groups showed the same gross results, 22 runs was a big enough sample. This is what happened, as is shown in figure 1. In this figure, the percentage of runs that resulted in an error (in absolute value) in ξ less than some value $\Delta\xi$ is shown as a function of $\Delta\xi$. Note that the standard deviation of ξ in the three different groups (indicated by arrows on the abscissa) agrees within about ±15 percent and that, in general, the three sets of results describe a similar curve. For reference a uniform distribution curve and a normal distribution curve which approximate the results are shown.

Effect of number of cycles and points per cycle on $SD\xi$.- Shown in figure 2 is the standard deviation in ξ, $SD\xi$, versus the number of observed cycles of motion for several values of N (observation points per cycle). These results are for the case where the exact value of ξ is zero. Note that $SD\xi$ increases rapidly below 1-1/2 cycles of motion. Furthermore the effect of N is generally small for values of N greater than about 4. The theoretical curve for the simple two point theory is shown by the upper solid line. It appears to have the proper dependence on n for values of n greater than about 1-1/2; however, the level of the curve is too high in this range. The fact that the shape of the curve is not predicted by the simple theory for values of n less than 1-1/2 is not too surprising since there are fewer than three peaks in the pitching motion and the data reduction procedure has difficulty distinguishing between trim and damping. Also shown in the figure are two curves besides the simple theory curve; one of these is the simple theory adjusted by a constant to

give the best fit to the results. The other curve is an exponential which gives a better fit over the range of variables considered but has no theoretical justification, as is indicated by the fact that it approaches a nonzero asymptote.

Effect of ξ on $SD\xi$.- Since the results in figure 2 were obtained for $\xi = 0$, it was of interest to see if the simple theoretical model which indicated that the $SD\xi$ was independent of ξ did indeed hold. Recall that for large values of ξ the amplitude change can be large and thus the relative error in α, $SD\alpha/\alpha_{env_O}$ will be different at different points along the trajectory. Therefore in considering the results for large values of ξ it would seem logical that the results should be compared for the same value of $SD\alpha/\alpha_{RMS}$ where α_{RMS} is the root-mean-square angle of attack over the trajectory. Shown in figure 3 are results for various values of ξ. The solid points are the results as obtained for a constant value of $SD\alpha/\alpha_{env_O}$. Note there may be a slight effect of ξ on the $SD\xi$. The open points are the same results corrected to the same value of $SD\alpha/\alpha_{RMS}$ as in the case of $\xi = 0$. The correction was made using the linear approach suggested by the simple theory. This simple correction does appear to reduce the small effect of ξ_E on the $SD\xi$. It is therefore felt that for most practical cases $SD\xi$ is essentially independent of ξ.

Effect of $SD\alpha$ on $SD\xi$.- In figure 4 the $SD\xi$ is plotted versus $SD\alpha/\alpha_{RMS}$ for a series of different conditions. Both $SD\alpha$ and α_{RMS} were varied, as well as the type of error function used to generate

the errors in α. The correlation about a straight line is very good, thus supporting the simple theoretical model. In addition to these considerations a group of runs was treated as though every station had been read twice and both sets of readings analyzed as one run. Theoretically this should be equivalent to reducing $SD\alpha$ by $1/\sqrt{2}$. This is indeed realized as shown by the triangular data points. The solid point is the result as obtained; the open point has been shifted by $1/\sqrt{2}$, which brings it back to the curve.

Effects of $m/\rho A\lambda$ and SDx on $SD\xi$.- Several different groups of 22 runs were considered with different values of $m/\rho A\lambda$. All of these groups showed excellent agreement with the simple theoretical model.

In addition to the errors in α, errors were also introduced into x. The effect of errors in x was so small as to be hardly detectable. Therefore all of the results that have been presented included errors in x of up to 0.006 inch.

Estimation of $SD\xi$.- Combining all of the previous results it is possible to write an equation which expresses $SD\xi$ in terms of all the variables considered. This equation can be expressed as:

$$SD\xi = C\left(\frac{m}{\rho A\lambda}\right)\left(\frac{SD\alpha}{\alpha_{RMS}}\right) f(n) \qquad (12)$$

where C is a constant and $f(n)$ is a function which describes the effect of the number of cycles. If we take the function $f(n)$ as that given by the simple theoretical model, equation (12) can be written as:

$$SD\xi = 1.70\left(\frac{m}{\rho A\lambda}\right)\left(\frac{SD\alpha}{\alpha_{RMS}}\right)\left(\frac{1}{n}\right) \qquad (13)$$

On the other hand if we take the best fit to all the data given in figure 2 we get the equation

$$SD\xi = 0.183\left(\frac{m}{\rho A\lambda}\right)\left(\frac{SD\alpha}{\alpha_{RMS}}\right)e^{\frac{3.07}{n}} \qquad (14)$$

Either one of these equations can be used to estimate the standard deviation ξ.

It should be noted that these equations do not include the effect of the number of observation points per cycle (N) as it is generally quite small. Its influence, however, was systematic in that the more points per cycle the better were the results. It would require considerably more statistical results to adequately define the functional effect of this parameter over the range of variables considered; however, it would be a relatively simple matter to apply the procedure outlined to a given test facility.

Implications of equation (13).- At first glance equation (13) would appear to indicate that the best results would be obtained with the most cycles, and this would be true except that usually the term $1/n$ is not truly independent of $m/\rho A\lambda$. If we substitute $n\lambda = x$, where x is the length of the testing range, we get

$$SD\xi = 1.70\left(\frac{m}{\rho Ax}\right)\left(\frac{SD\alpha}{\alpha_{RMS}}\right) \qquad (15)$$

Therefore the longer the facility the smaller $SD\xi$. For a given facility x is fixed; therefore we minimize $SD\xi$ by minimizing $m/\rho A$, being sure that we have more than 1-1/2 cycles. A good optics system yielding a clear image will also minimize errors in angle readings (i.e., reducing $SD\alpha$) thus minimizing $SD\xi$. This may require resorting to

Kerr cells for very high speed tests to reduce blur and to reduce fogging due to model radiation. One can also make multiple readings of each picture to reduce SD_α. However, this will not work unless the errors are truly random. Errors that are not random deserve attention also. Examples of factors which can introduce nonrandom error are the facility reference system, dimensional stability of the film used, extraneous "noise" on the film, and uncorrected optical distortion either in the optics or due to refraction. The use of focussed shadowgraphs can minimize the effect of refraction.

Effect of random experimental errors on the determination of λ.- For all of the cases considered the errors in the determination of λ were less than 1/2 percent. As in the case for damping, the number of cycles of motion had a significant influence on this error. This effect of the number of cycles is shown in figure 5. Note the similar appearance to that shown for SD_ξ in figure 2. Since the errors are so small, this subject was not considered any further.

ANALYSIS OF VARIOUS ASSUMPTIONS

As was stated earlier two assumptions which appear to affect the dynamic stability parameter to a considerable degree are: (1) the resultant angle of attack is the square root of the sum of the squares of the projected angles instead of $\alpha_r = \tan^{-1}\sqrt{\tan^2 \alpha + \tan^2 \beta}$; and (2) the aerodynamics are linear. The method of analysis that follows is similar to that in the previous section except that no random experimental errors are introduced.

Analysis of the Resultant Angle-of-Attack Assumption

This effect was studied by considering a planar trajectory which is observed at different angles of rotation, φ, with respect to the plane of the motion (see sketch (b)).

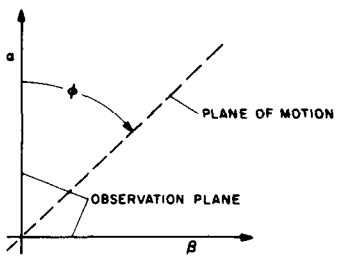

Sketch (b)

Note that for $\varphi = 0^\circ$ or 90° there is no assumption because $\alpha_r = \alpha$ or $\alpha_r = \beta$. To illustrate the magnitude of error that this assumption can introduce at intermediate values φ we will consider a particular example. For our example we will take 11 stations at 4-foot intervals, $\rho A/m = 0.006/\text{ft}$ and $\lambda = 25.7$ ft. We consider various values of α_{RMS}, φ, and ξ.

Figure 6 shows the results of this analysis for three values of the dynamic stability parameter, ξ. Plotted here are the apparent values of ξ as a function of φ for various values of α_{RMS}. Note that both α_{RMS} and φ have a strong influence on ξ. Note further that this effect is a strong function of the size of ξ_E. Figure 7 shows the induced errors $(\xi - \xi_E)$ for $\varphi = 45^\circ$ as a function of ξ_E for two values of α_{RMS}. Note the nearly linear dependence of the induced error on ξ_E. Remember that here we are considering <u>exact</u> angle readings and that these errors are introduced by the method of analysis.

These errors can be eliminated completely for planar motion by a simple rotation of coordinates before the data are analyzed. Furthermore for motions which are not planar the influence of this assumption can be minimized by rotating the coordinate system so that most of the angular motion is confined to either the α or the β plane.

Analysis of the Assumption of Linear Aerodynamics

In many cases of practical interest the aerodynamic coefficients are nonlinear functions of angle of attack; the question then arises as to the relationship that exists between the quasi-linear values obtained from the present data reduction procedure and the true values. Nonlinear moments with zero damping have received considerable attention (e.g., refs. 2 and 3). The more complicated cases have received little or no attention.

Here we will consider a slightly more complicated case, that is, $\xi = \text{const} \neq 0$, and $-C_m = M_0\alpha + M_2\alpha^3$. Again <u>exact</u> planar trajectories, with 11 stations at 4-foot intervals, will be used. Two cases are considered; in both, M_0 gave a stabilizing moment. One case had M_2 stabilizing and one had M_2 destabilizing, referred to as stable-stable and stable-unstable, respectively.

Results of Linear Aerodynamic Assumption

Two questions are of interest here. First, does the nonzero damping significantly affect the determination of the nonlinear pitching

moments as outlined by Rasmussen and Kirk (ref. 3)? Second, does the presence of the nonlinear moment significantly affect the measured value of ξ?

For the amounts of damping considered here there was no detectable influence of $\xi \neq 0$ on the nonlinear pitching moment (i.e., the correct pitching-moment curve could be determined using the existing data reduction procedure in conjunction with the method of Rasmussen and Kirk).

This was not usually true for determining the damping. Here the nonlinear moment had a large influence on the damping determined with the present data reduction procedure. These results are shown in figure 8. The circles are the results for a pitching moment which is stable-stable. The scatter is due to the finite number of observation stations. Similar results for a stable-unstable pitching moment are indicated by squares. The sign of the nonlinear term determines whether the observed value of ξ will be larger or smaller than the exact value and that the angle of attack (more precisely the quantity $M_2\alpha^2$) determines the magnitude of the difference between apparent and exact values of ξ. The size of the nonlinearities considered are given in the figure.

Note particularly what this figure demonstrates. A system has been defined where the damping parameter, ξ, is a constant. However, after the analysis ξ appears to be a function of amplitude. Care must be taken that these effects of the nonlinear moment on the damping are interpreted correctly, and some theoretical work toward this end has been done.

Theoretical comparison.- Also shown in figure 8 are some theoretical estimates of the degree of interaction of a nonlinear moment on ξ. This work was done by Maurice Rasmussen and supplied by private communication. His analysis starts by assuming that the nonlinearity is small. A perturbation solution can then be obtained showing the effect of the nonlinearity in the moment. The theory gives the correct trend but not necessarily the correct magnitude. The work of Rasmussen is being expanded and will be published in the near future.

REFERENCES

1. Nicolaides, John D.: On the Free Flight Motion of Missiles Having Slight Configurational Asymmetries. BRL Rep. 858, Aberdeen Proving Ground, 1953. Also IAS Preprint 395, 1953.

2. Kirk, Donn B.: A Method for Obtaining the Nonlinear Aerodynamic Stability Characteristics of Bodies of Revolution From Free-Flight Tests. NASA TN D-780, 1961.

3. Rasmussen, Maurice L.; and Kirk, Donn B.: On the Pitching and Yawing Motion of a Spinning Symmetric Missile Governed by an Arbitrary Nonlinear Restoring Moment. NASA TN D-2135, 1964.

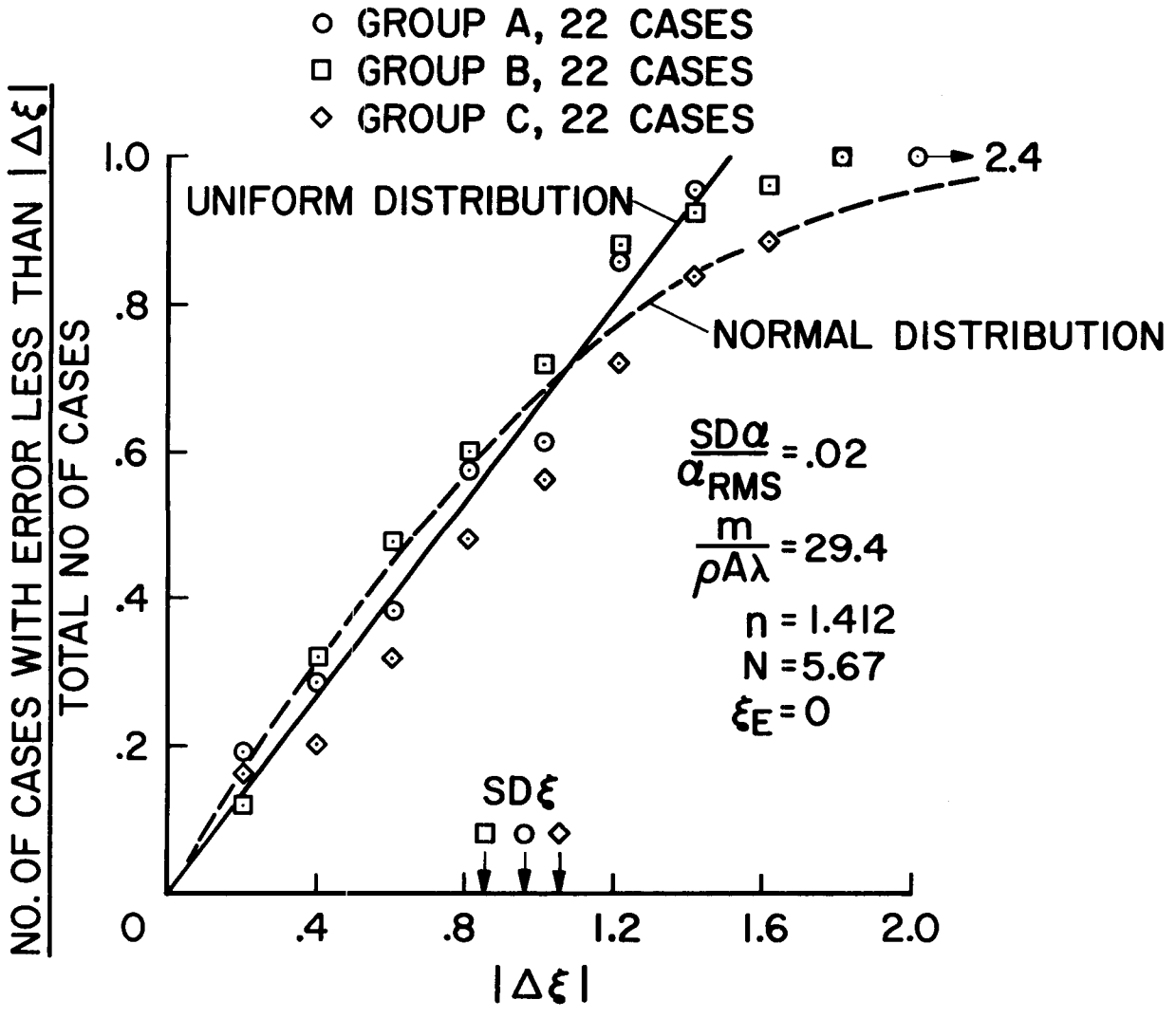

Figure 1.- Comparison of results from three groups of 22 trajectories each.

NATIONAL AERONAUTICS AND SPACE ADMINISTRATION
AMES RESEARCH CENTER, MOFFETT FIELD, CALIFORNIA

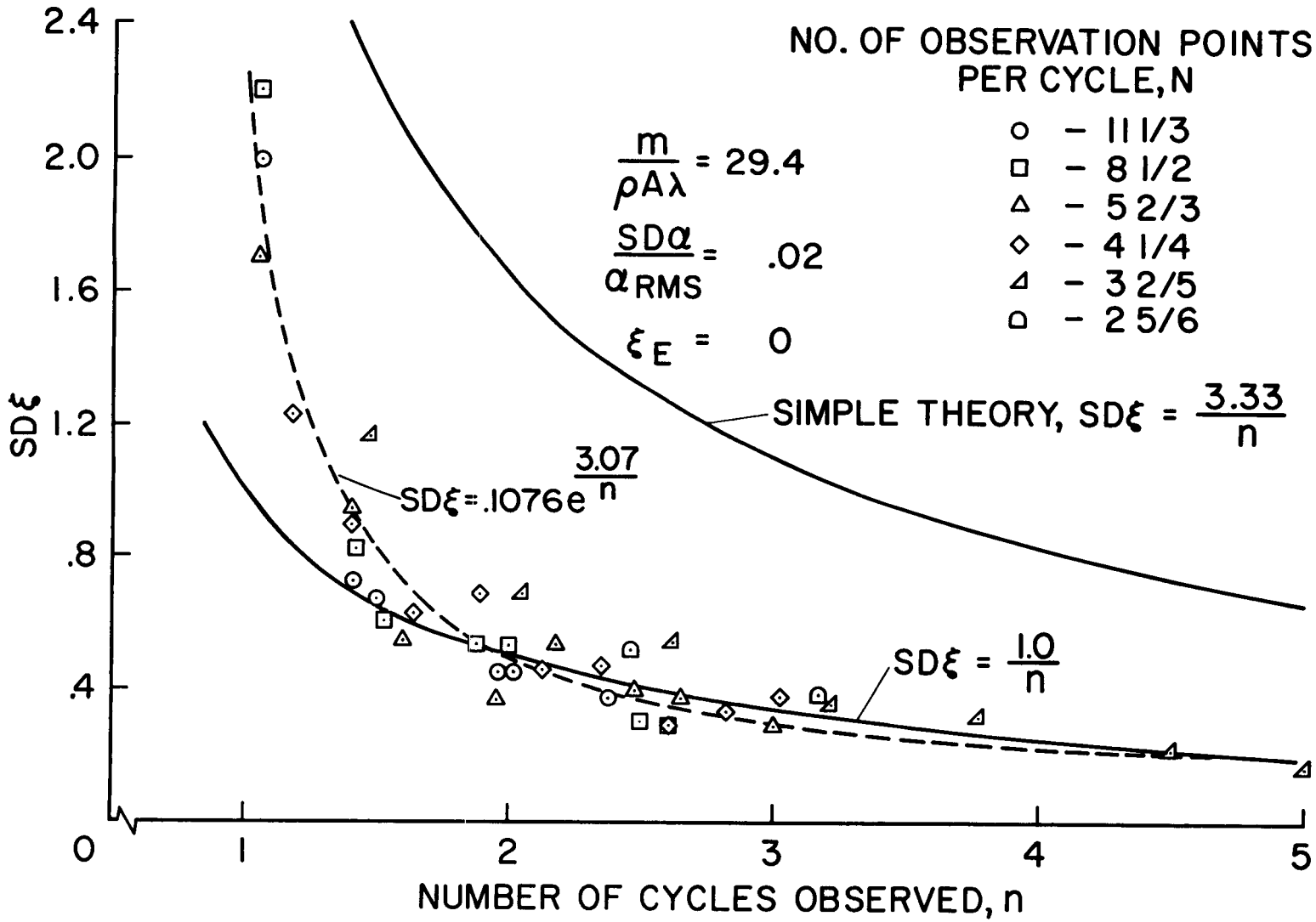

Figure 2.- Effect of n and N on the standard deviation in the dynamic stability parameter.

NATIONAL AERONAUTICS AND SPACE ADMINISTRATION
AMES RESEARCH CENTER, MOFFETT FIELD, CALIFORNIA

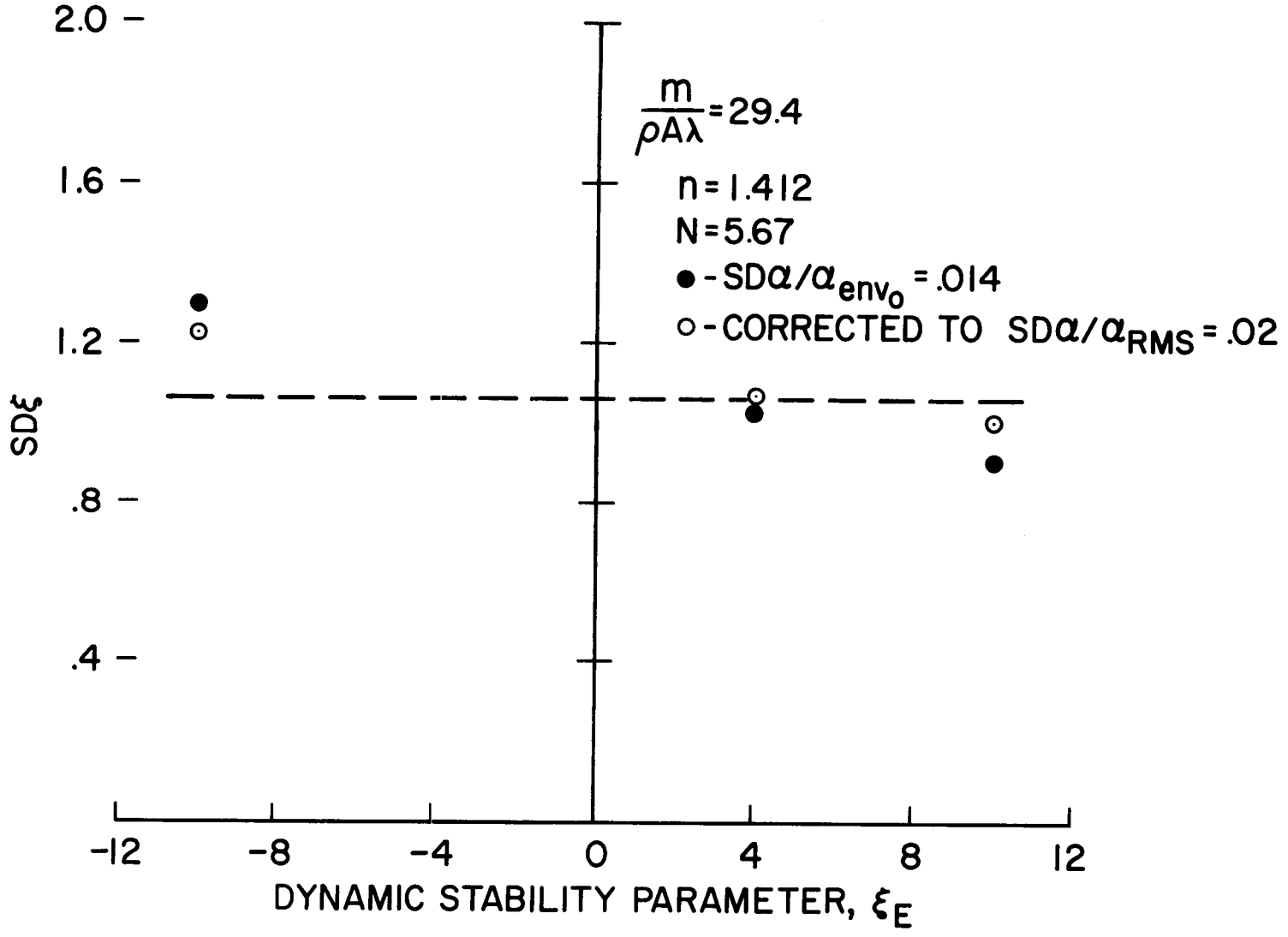

Figure 3.- Effect of the absolute level of the dynamic stability parameter on SDξ.

NATIONAL AERONAUTICS AND SPACE ADMINISTRATION
AMES RESEARCH CENTER, MOFFETT FIELD, CALIFORNIA

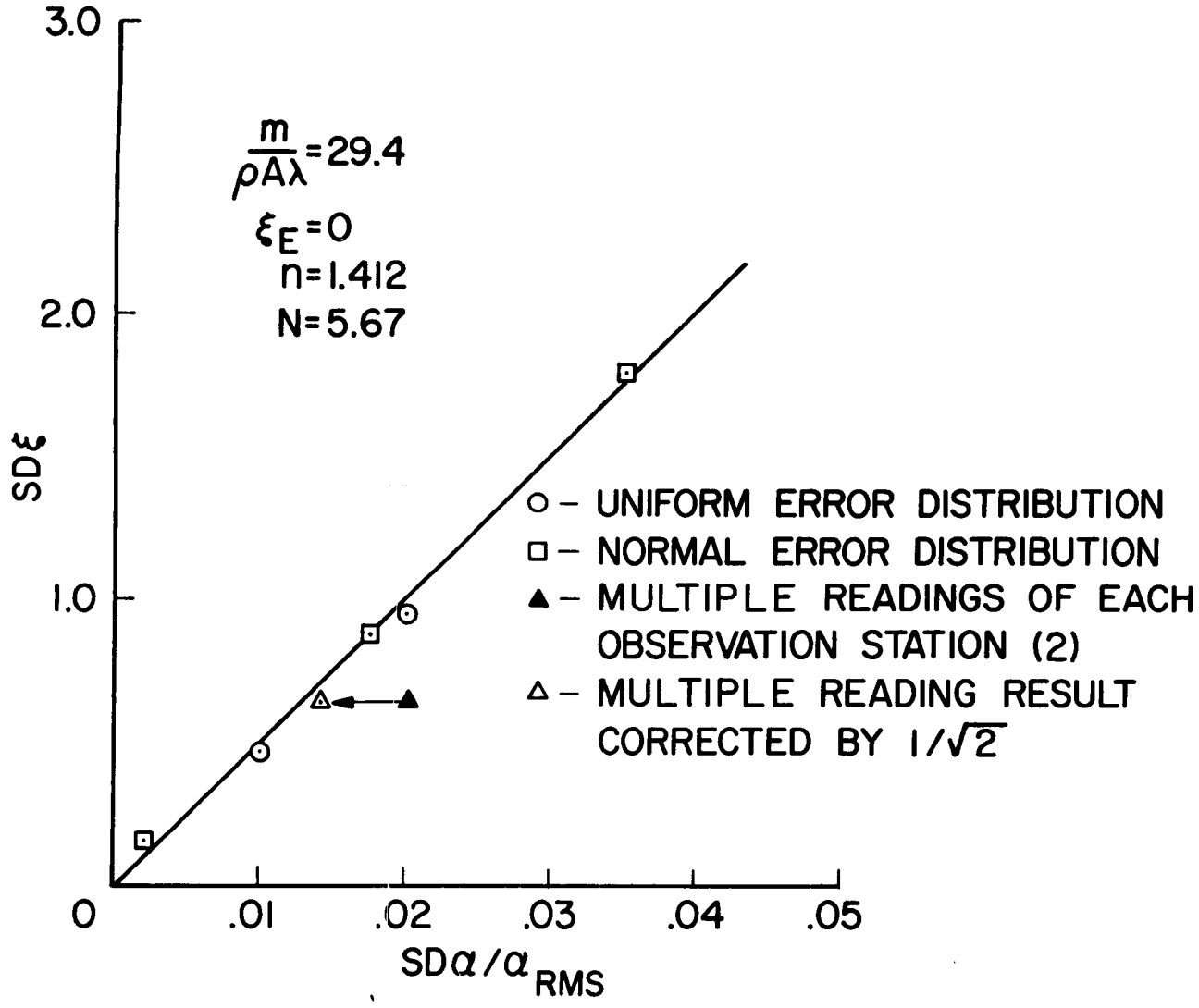

Figure 4.- Effect of SDα on SDξ.

NATIONAL AERONAUTICS AND SPACE ADMINISTRATION
AMES RESEARCH CENTER, MOFFETT FIELD, CALIFORNIA

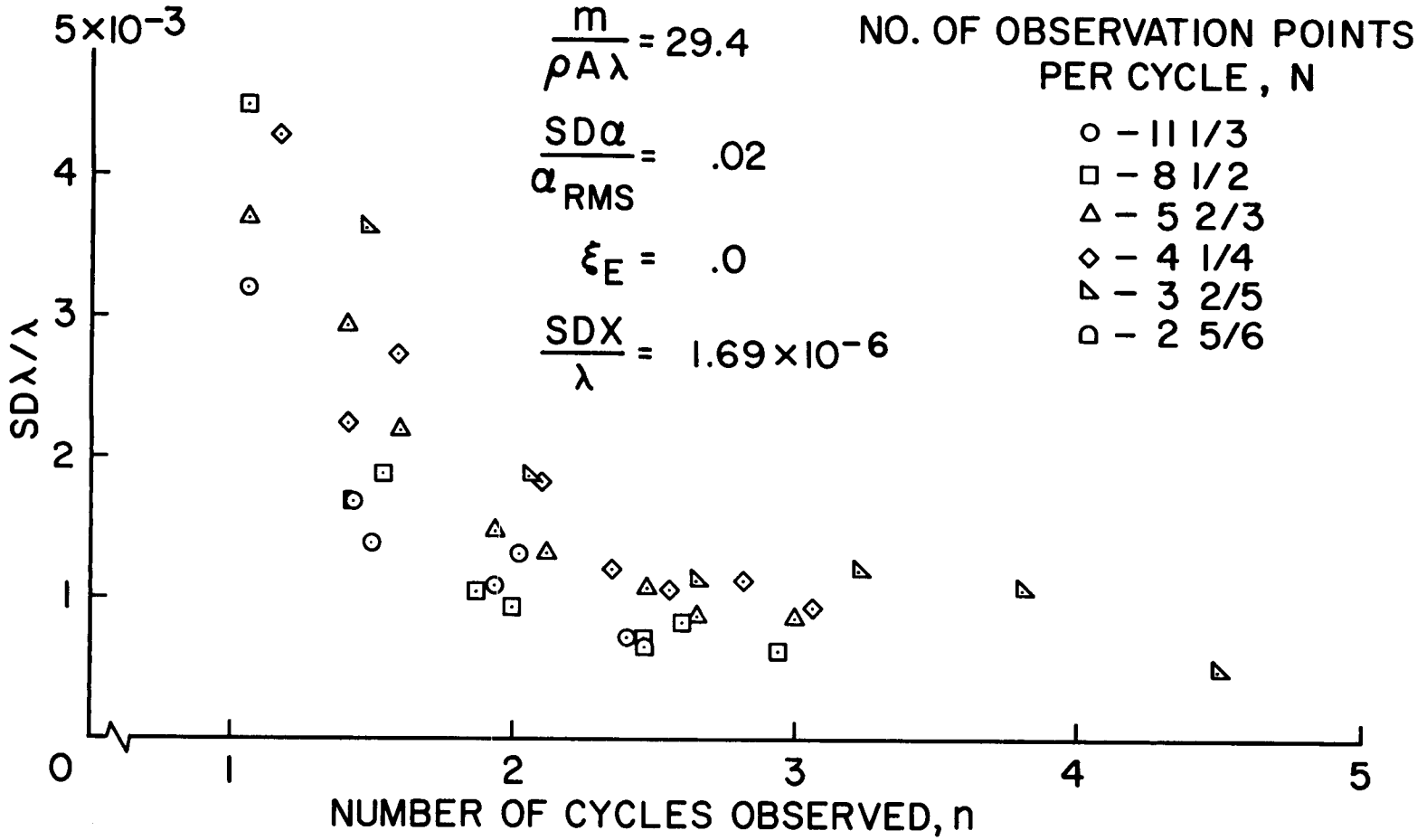

Figure 5.- Effect of n and N on the standard deviation in the wave length.

NATIONAL AERONAUTICS AND SPACE ADMINISTRATION
AMES RESEARCH CENTER, MOFFETT FIELD, CALIFORNIA

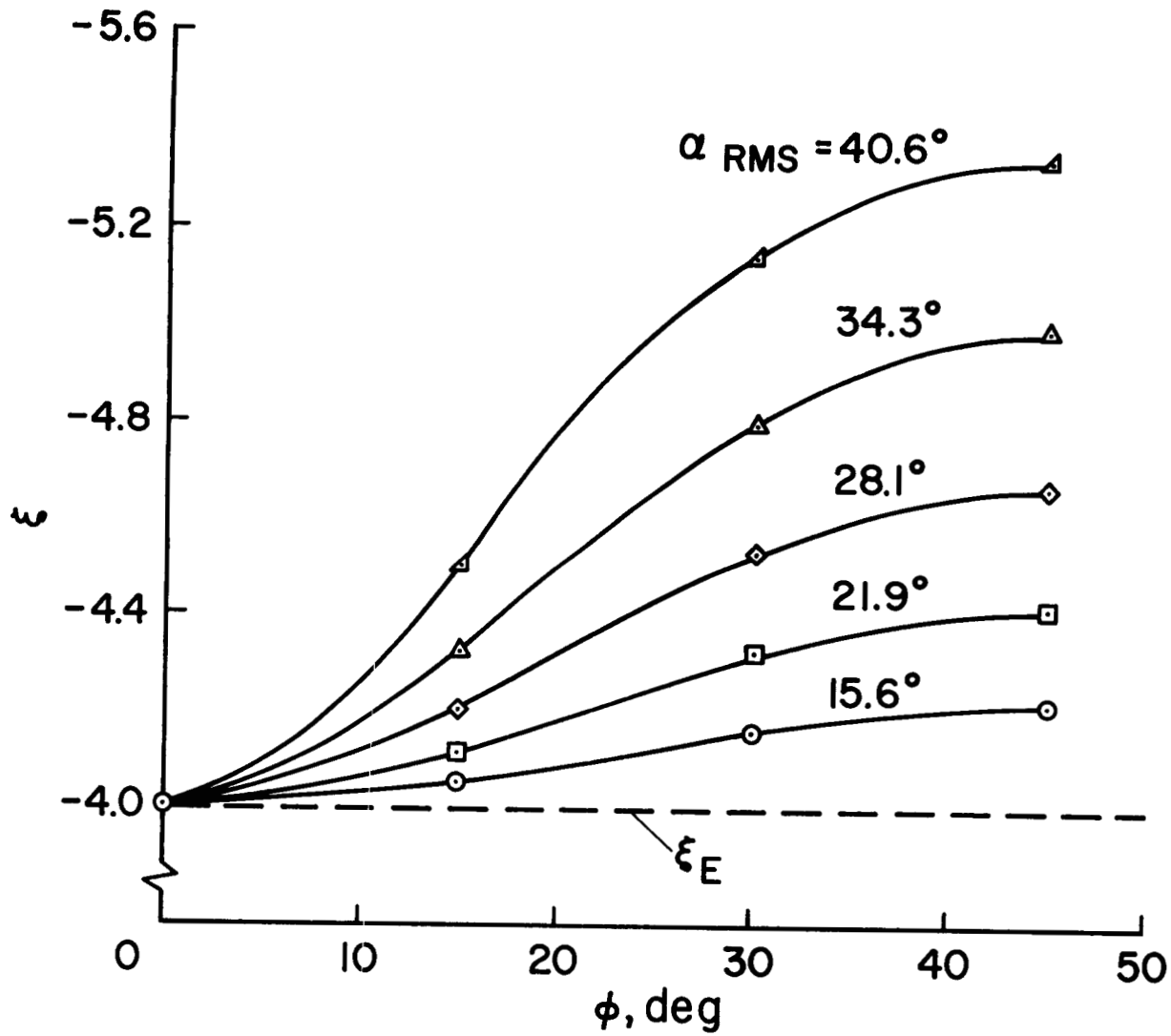

(a) ξ (exact) = -4.0

Figure 6.- Errors induced in the dynamic stability parameter by small angle assumption.

NATIONAL AERONAUTICS AND SPACE ADMINISTRATION
AMES RESEARCH CENTER, MOFFETT FIELD, CALIFORNIA

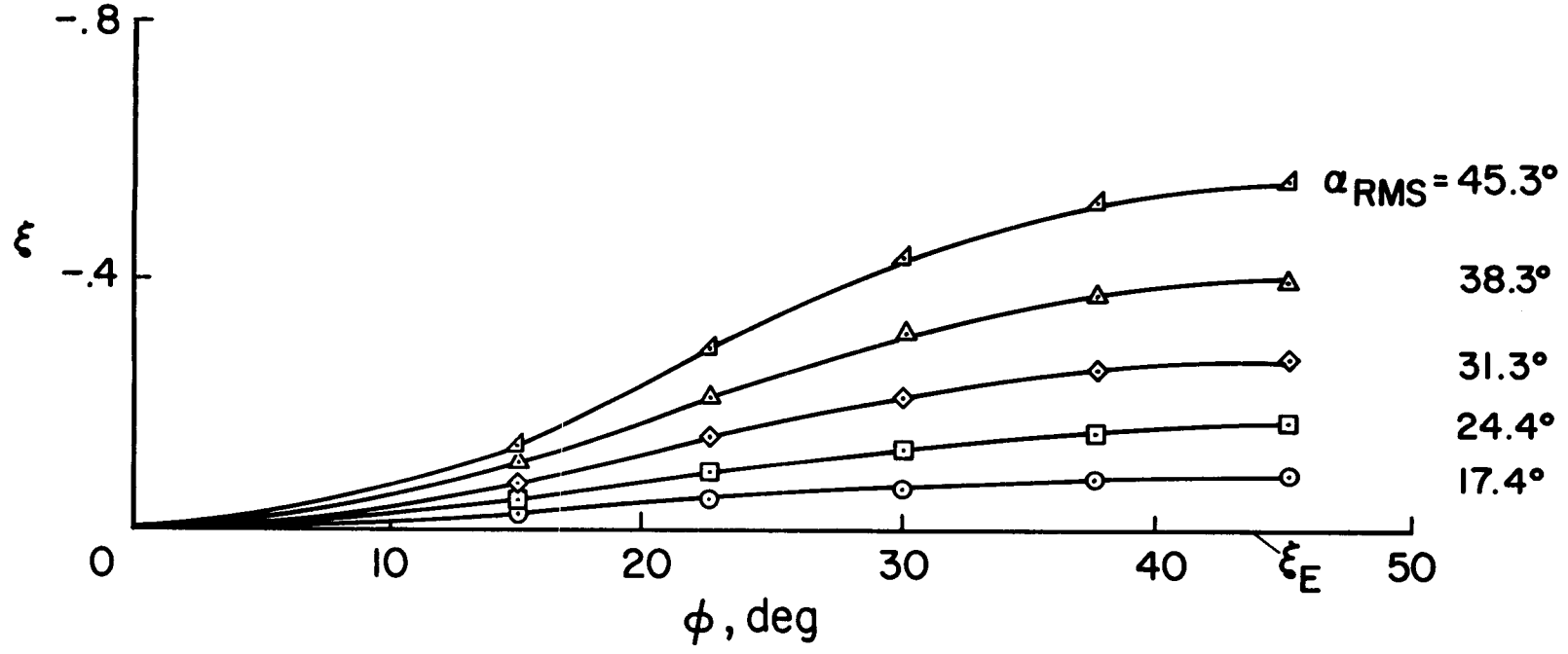

(b) ξ (exact) = 0

Figure 6.- Continued.

NATIONAL AERONAUTICS AND SPACE ADMINISTRATION
AMES RESEARCH CENTER, MOFFETT FIELD, CALIFORNIA

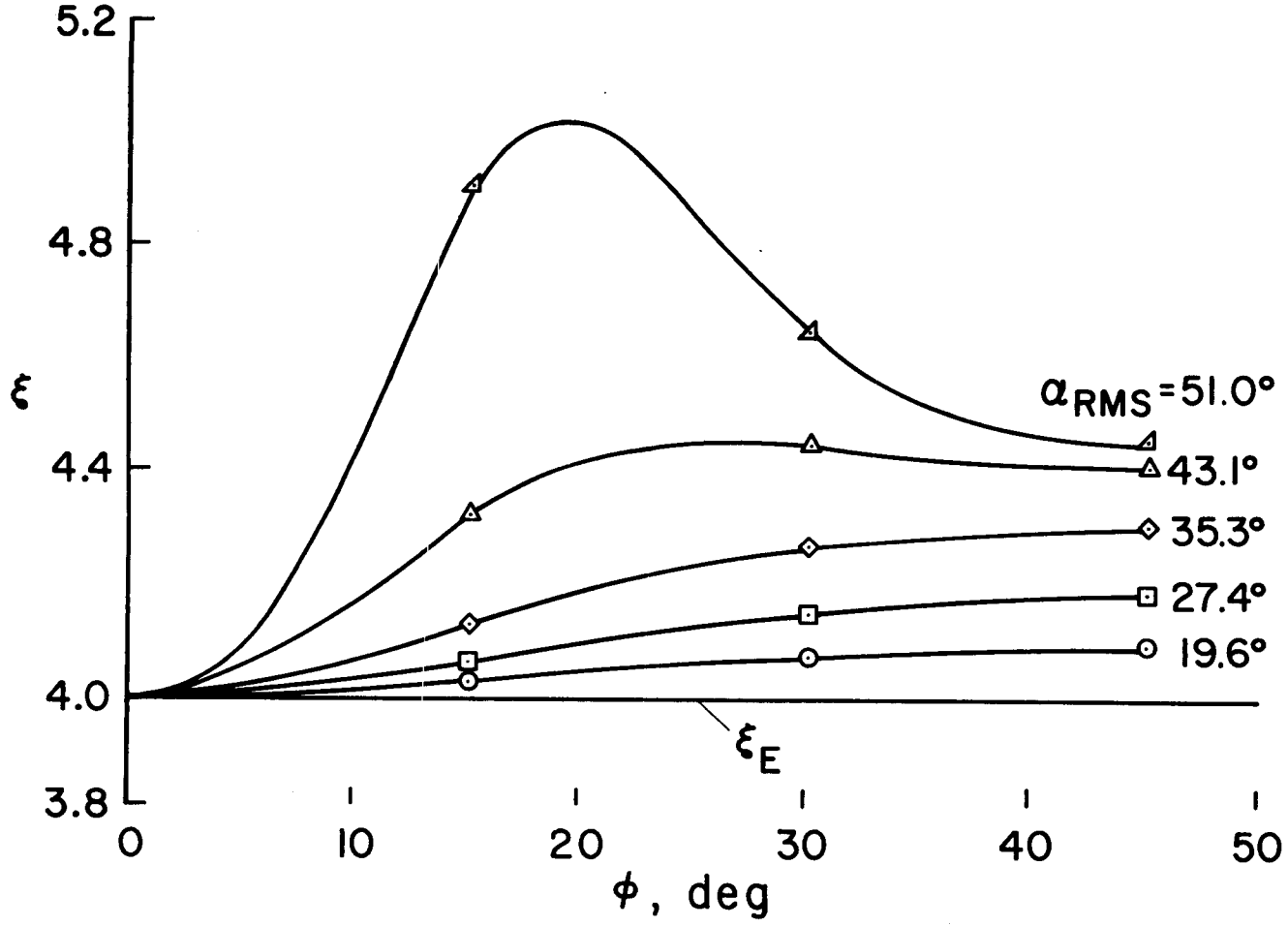

(c) ξ (exact) = 4.0

Figure 6.- Concluded.

NATIONAL AERONAUTICS AND SPACE ADMINISTRATION
AMES RESEARCH CENTER, MOFFETT FIELD, CALIFORNIA

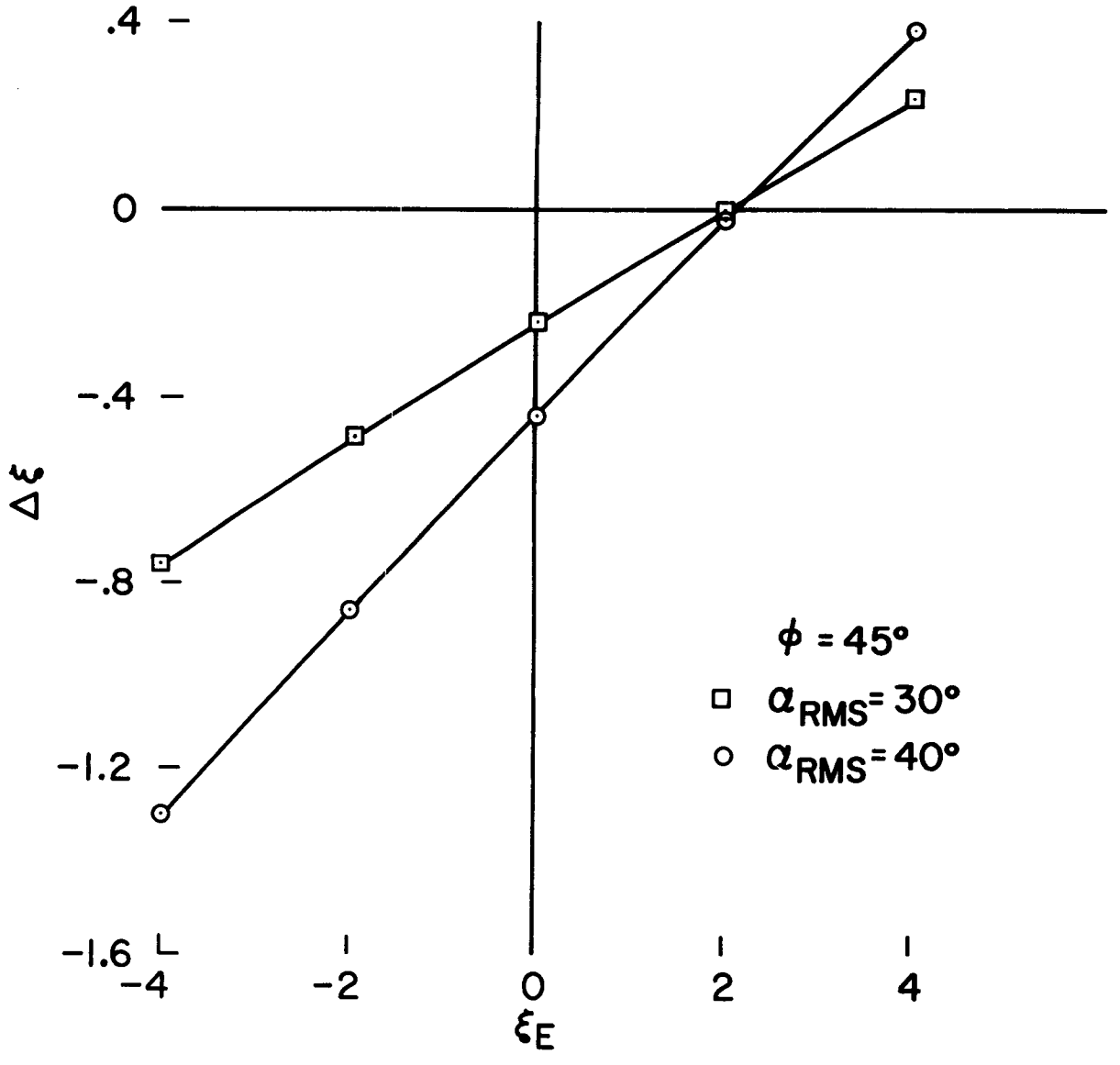

Figure 7.- Cross plot showing effect of the absolute level of the dynamic stability parameter on induced errors.

NATIONAL AERONAUTICS AND SPACE ADMINISTRATION
AMES RESEARCH CENTER, MOFFETT FIELD, CALIFORNIA

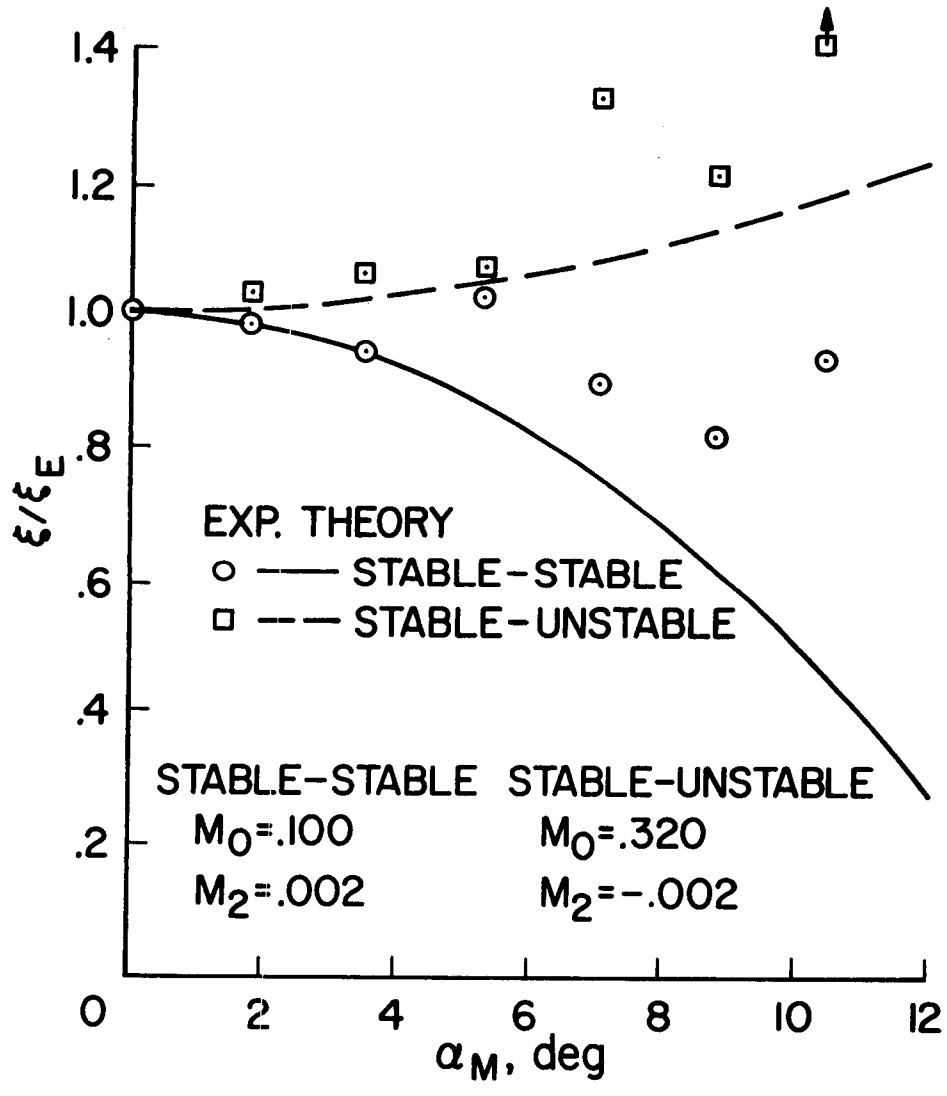

Figure 8.- Effect of nonlinearities in the restoring moment on deduced values of the dynamic stability parameter.

NATIONAL AERONAUTICS AND SPACE ADMINISTRATION
AMES RESEARCH CENTER, MOFFETT FIELD, CALIFORNIA